Journal of the Serbian Chemical Society
JSCS@tmf.bg.ac.rs • www.shd.org.rs/JSCS
J. Serb. Chem. Soc. *90* (6) 767–780 (2025)
JSCS–5419
Original scientific paper
Published 24 June, 2025

Catalytic performance of palladium/degraded chitosan for acetylene selective hydrogenation

SI-YE TANG[1]*, XIN-XIANG CAO[1]**, TONG-TONG DI[2] and XIN-YU LI[3]

[1]College of Chemistry and Chemical Engineering, Luoyang Normal University, Luoyang 471934, China, [2]School of Chemical Engineering, Northwest University, Xian 710069, China and [3]School of Chemical Engineering, Zhengzhou University, Zhengzhou 450001, China

(Received 19 December 2024, revised 31 January, accepted 27 April 2025)

Abstract: The aim of this paper was to investigate the catalytic properties of palladium supported on chitosan catalysts. The effect of primitive chitosan and degraded chitosan on catalytic performance was compared. The structure, morphology, metal content and properties of the catalysts were characterized by Fourier transform infrared spectroscopy (FTIR), scanning electron microscopy (SEM), inductively coupled plasma spectrometry (ICP), X-ray diffraction (XRD), Brunauer–Emmett–Teller (BET) method and X-ray photoelectron spectroscopy (XPS). The results showed that the catalytic performance of Pd/degraded chitosan was better than that of Pd/chitosan at a certain Pd load. Pd/degraded chitosan (degradation 4 h) catalyst exhibited excellent catalytic performance and stability. The acetylene conversion and ethylene selectivity, respectively, achieved 100 and 91 %. During 13.5 h, the acetylene conversion maintained 100 % and the ethylene selectivity decreased slightly from 88 to 71 %. Based on this study, it was demonstrated that Pd was successfully coordinated with chitosan; after degradation, the chitosan particles became smaller and had larger surface areas; these were conducive to improve the catalytic performance of Pd/degraded chitosan. Pd/degraded chitosan also had high selectivity at high conversion, greatly improving the characteristics of low selectivity at high conversion of traditional Pd-based catalysts.

Keywords: chitosan; conversion; degradation; selectivity.

INTRODUCTION

A significant proportion of ethylene is produced from naphtha cracking.[1] This process makes ethylene to be contaminated with 0.5–2 % of acetylene, which can poison the Ziegler–Natta catalyst used for downstream ethylene polymerization.[1] Selective hydrogenation of small amounts of acetylene in ethylene

* Corresponding authors. E-mail: (*)tsy6611@163.com; (**)xiangzi827@163.com
https://doi.org/10.2298/JSC241219031T

rich feedstocks is an important industrial target. Namely, acetylene is effectively removed from ethylene via hydrogenation to ethylene. At the same time, substantial hydrogenation of ethylene and over-hydrogenation of acetylene to undesirable ethane are avoided. In order to avoid poisoning of the catalyst in the ethylene polymerization, acetylene concentration must be reduced to a level less than 5 ppm.[1] So it is necessary to seek the catalysts with both high activity for acetylene conversion and high selectivity for ethylene. The traditional industrial catalysts are Pd-based systems, which usually show a poor selectivity at high conversion of acetylene.[1,2] How to improve the selectivity of Pd-based catalysts has always been the focus of researchers.

It is well known that catalyst support strongly influences the catalytic performance of Pd.[3–6] Changing support is one of the effective methods to improve the catalytic performance of a catalyst. In industry, Al_2O_3, SiO_2 and carbon are commonly used as supports of Pd-based catalysts for acetylene selective hydrogenation.[7–9] As a biodegradable materials, polysaccharides have gained lot of attention in the synthesis of catalysts.[10] These biodegradable resources can decrease the utilization of non-renewable materials and minimize the environmental pollution. Chitosan (CS) is classified as polysaccharides, obtained from chitin which is the second most abundant natural polymer present on the earth.[11] Duo to the hydroxyl and amino groups, CS has strong affinity for metal ions and high sorption capacities for catalytic metals such as palladium, copper, platinum. It has been shown to be a very promising support.[12,13] Researchers used Pd supported on CS (or CS derivatives) as catalysts for oxidation reactions, hydrogenation reactions, allylic substitution reactions, carbonylation reactions, Suzuki and Heck reactions.[12] For the hydrogenation reaction, Jin used silica-supported CS––Pd catalysts for the hydrogenation of nitrobenzene, 1-hexene, acrylic acid, chloronitrobenzene and phenol to aniline, hexane, propionic acid, chloroaniline and cyclohexanone, respectively.[12] However, Pd/CS composites have not yet been used as catalysts for acetylene selective hydrogenation in the available literature so far.

In this work, we utilized CS to prepare Pd-based catalysts. The catalytic properties of the obtained catalysts were tested by selective hydrogenation of acetylene. In addition, the stability of the resultant catalyst was also studied. Simultaneously, the obtained catalysts were characterized by X-ray diffraction (XRD), scanning electron microscopy (SEM), inductively coupled plasma spectrometry (ICP), Brunauer–Emmett–Teller (BET) method, Fourier transform infrared spectroscopy (FTIR) and X-ray photoelectron spectroscopy (XPS).

EXPERIMENTAL

Materials

CS (pharmaceutical grade, deacetylation degree: 80–95 %) was purchased from Sinopharm Chemical Reagent Co., Ltd. (Shanghai, China). All the other reagents were purchased

from Damao Chemical Reagent Factory (Tianjin, China). They were of analytical grade and were used without further purification.

Preparation of the degraded CS

2 g of CS was put into a 250 mL round bottom flask. 100 mL of 2 % acetic acid aqueous solution was added to the flask. The suspension was then magnetically stirred at 30 ℃ for 4 h to ensure CS complete dissolution. 8 mL of 30 % H_2O_2 aqueous solution was added to the CS acetic acid solution. The above mixed solution reacted at 50 ℃ for 6 h under stirring.

Then the pH of reaction mixture was adjusted to be neutral using 1 M NaOH aqueous solution. The product was separated by centrifugation (10000 rpm for 5 min) and washed three times with distilled water and anhydrous ethanol, respectively. Then the product was dried in an oven at 40 ℃ for 12 h. The degraded CS sample was obtained. The degradation time was set to 0.5, 1, 2, 4 and 6 h. The corresponding CS samples were labeled as degraded CS (0.5 h), degraded CS (1 h), degraded CS (2 h), degraded CS (4 h) and degraded CS (6 h), respectively.

Measurement of intrinsic viscosity ([η]) of CS

The value of [η] can reflect the molecular weight of a polymer. The smaller the [η], the smaller the molecular weight. A certain amount of CS sample was dissolved into 20 mL of formic acid. The [η] of CS sample was determined using Obblehode viscometry. The values of [η] were calculated according to the literature method.[14]

Preparation of Pd/CS and Pd/degraded CS

0.6 g of CS (or degraded CS) was put into a 250 mL round bottom flask. 100 mL of 2 % acetic acid aqueous solution was added to the flask. The suspension was then magnetically stirred at 50 ℃ until the CS (or degraded CS) was completely dissolved. A certain volume of $PdCl_2$ hydrochloric acid solution was added dropwise to the CS (or degraded CS) solution under stirring. The mixture reacted at 60 ℃ for 2 h.

Then the reaction mixture was cooled and adjusted to be neutral using 1 M NaOH aqueous solution. The product was separated by centrifugation (10000 rpm for 5 min) and washed three times with distilled water. Then the product was dried at 40 ℃ to constant weight. The dried sample was Pd/CS (or Pd/degraded CS) catalyst.

Catalytic performance experiment

Pretreatment before reaction. 30–31 mg of catalyst was put into a quartz tube reactor (4 mm inner diameter). The quartz tube reactor was fixed in an oven with a programmed temperature controller. The catalyst was reduced in situ for 2 h under a flow of H_2/Ar mixture at 130 ℃ by heating from room temperature using a heating rate of 5 ℃ min^{-1}. The volume ratio of H_2 to Ar was 1 to 3. Then the reactor was cooled down to the reaction temperature under the protection of Ar gas.

Selective hydrogenation of acetylene. Ar, H_2 and feed gas mixture of 94.95 % C_2H_4, 5.05 % C_2H_2 were continuously introduced into the quartz tube reactor. The total flow rate of Ar, H_2, C_2H_4 and C_2H_2 mixture was 30 mL min^{-1} and the volume ratio of H_2 to C_2H_2 was 20 to 1. The total gas hourly space velocity (*GHSV*) was 60000 mL h^{-1} g^{-1}. All gas flows in the reaction were controlled with mass flow controllers. The gas products from the reactor outlet were analyzed three times at each reaction temperature by an online gas chromatography (GC--2020, Tengzhou Zhongke spectrum analysis instrument Co. Ltd, Shandong, China) equipped with a flame ionization detector and a 30 m×0.32 mm (i.d.)×1.50 μm XP-Plot capillary column (column box temperature:100 ℃; detector temperature: 200 ℃). The analysis data of

the gas chromatography was collected using a PC work-station. These analysis data that included the amount of C_2H_2, C_2H_4 and C_2H_6 in the gas products from the reactor outlet were used to calculate the conversion and selectivity of the catalyst. Acetylene conversion and selectivity to ethylene were calculated as follows:[1,15]

$$C_2H_2 \text{ conversion} = 100\frac{C_2H_2(\text{in feed}) - C_2H_2(\text{in products})}{C_2H_2(\text{in feed})} \quad (1)$$

$$C_2H_4 \text{ selectivity} = 100(1 - \frac{C_2H_6(\text{in products}) - C_2H_6(\text{in feed})}{C_2H_2(\text{in feed}) - C_2H_2(\text{in products})}) \quad (2)$$

Characterization

The actual metal load of the different catalysts was measured using ICP (Aglient 7800, USA). The structures of samples were investigated by FTIR (Invenio S, Germany) using KBr disk technique. Each spectrum of the samples was acquired by accumulation of 27 scans with a resolution of 4 cm^{-1}. Morphology of samples was characterized by SEM (Carl Zeiss Sigma 500, Germany). The compositions' phases of the as-prepared materials were identified by a XRD (Bruker D8 Advances, Germany) equipped with CuKα radiation (λ = 1.5418 Å) and operated at 40 kV and 40 mA with a 5° min^{-1} scan rate. The scanning angular range of 2θ was performed from 5 to 90°. The surface area measurements of catalysts were conducted according to the BET method at –196 °C (Asap 2020 Plus HD88, USA). The samples were pretreated at 120 °C for 4 h. The total pore volume was evaluated by single point pore volume at a relative pressure of 0.99. The binding energy (*BE*) and the chemical state of elements were determined by XPS (K-Alpha, UK). Binding energies were calibrated using the C_{1s} peak (*BE* = 284.8 eV) as standard.

Before XRD and XPS analyses, the catalysts were reduced in situ for 2 h under a flow of H_2/Ar mixture at 130 ℃.

RESULTS AND DISCUSSION

The [η] of CS sample

The values of [η] are listed in Table I. As can be seen from Table I, the values of [η] decreased with degradation time. This indicates that the molecular chain of CS was broken and the molecular weight of CS was decreased.

TABLE I. The [η] of CS samples at different degradation time

Degradation time, h	0.0	0.5	1.0	2.0	4.0	6.0
[η] / mL g^{-1}	513.4	202.0	132.5	50.5	14.0	2.7

XRD analysis

XRD patterns of CS, degraded CS (4 h), 0.2 % Pd/CS and 0.2 % Pd/degraded CS (4 h) are shown in Fig. 1. 0.2 % indicates that the nominal load of the Pd is 0.2 mass %.

As shown in Fig. 1, the pattern of CS shows a broader and weaker characteristic peak at 2θ 24.0°. It indicates that the degree of crystallinity of CS was very low. A strong new characteristic peak appeared at 2θ 20.1° after degrading for 4 h. This suggests that the crystallinity of CS increased after degradation.

Crystallinity increase supports the theory that H_2O_2 solution penetrates and degrades the amorphous zone first.[16]

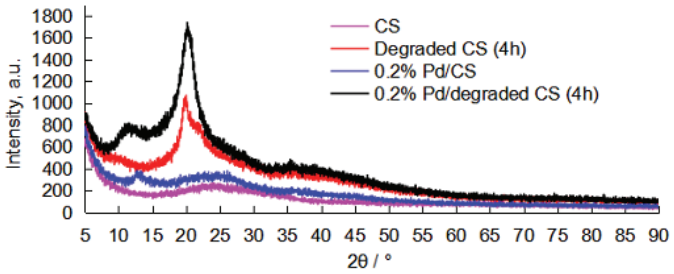

Fig. 1. XRD of CS, degraded CS (4 h), 0.2 % Pd/CS and 0.2 % Pd/degraded CS (4 h).

For 0.2 % Pd/CS and 0.2 % Pd/degraded CS (4 h) catalysts, due to the coordination of CS and degraded CS with Pd, both catalysts showed new absorption peaks at 2θ 12.8 and 11.7°, respectively.

Furthermore, no characteristic peak of Pd is observed in the XRD patterns of 0.2 % Pd/CS and 0.2 % Pd/degraded CS (4 h). This indicates that Pd species were amorphous and were uniformly dispersed. Perhaps the content of Pd was too low to be measured.

SEM analysis

Fig. 2 shows the SEM images of CS (Fig. 2a) and degraded CS (4 h) (Fig. 2b).

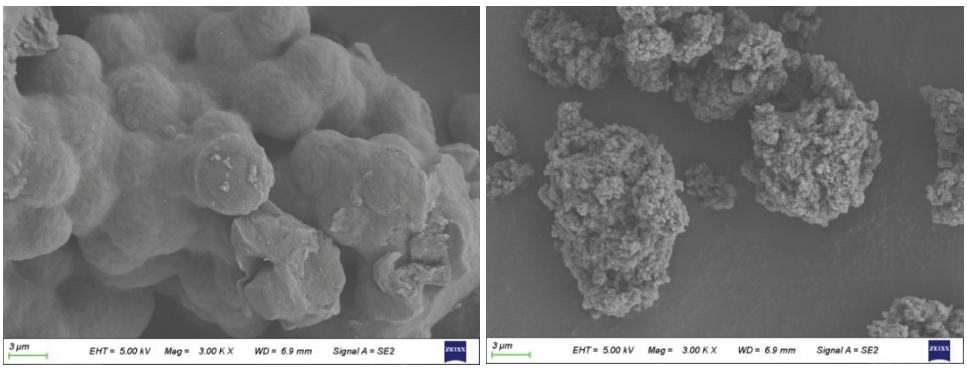

(a) (b)

Fig. 2. SEM image of: a) CS; b) degraded CS (4 h).

It can be seen that CS and degraded CS all presented uniform spherical particle and all had rough surface. However, the particle size of degraded CS was much smaller than CS. This was due to degradation of CS. Degradation made the molecular chain of CS break into small segments. The small particle size had

larger surface area. This was conducive to the dispersion of Pd and coordination of Pd with CS as well as improving catalytic performance.

ICP analysis

Actual load and the nominal load of Pd in Pd/CS and Pd/degraded CS (4 h) analyzed by ICP are summarized in Table II. It can be seen that the actual Pd load of Pd/degraded CS (4 h) was higher than that of Pd/CS. The reason was that the size of degraded CS was smaller than that of CS. Degraded CS with small size bound more readily with Pd. These results were in good agreement with the SEM results.

TABLE II. The Pd load, BET and total pore volume of catalysts

Catalyst	Nominal load of Pd, %	Actual load of Pd, %	Actual load of Pd after 13.5 h, %	BET surface area, m^2/g	Total pore volume, m^3/g
Pd/CS	0.20	0.13	0.13	2.14	0.017
Pd/degraded CS (4 h)	0.20	0.20	0.20	145.89	0.78

From Table II, the content of Pd was unchanged after reacting for 13.5 h. This demonstrates that the mass loss of catalyst was zero in the gas-solid phase catalytic reaction.

BET analysis

The BET surface areas of the samples are listed in Table II. The BET surface area of Pd/CS and Pd/degraded CS (4 h) are 2.14 and 145.89 m^2/g, respectively. The total pore volume of Pd/CS and Pd/degraded CS (4 h) are 0.017 and 0.78 cm^3/g, respectively. It can be seen that the surface area and pore volume of Pd/degraded CS (4 h) are higher than that of Pd/CS. The values of BET surface area confirmed that small particle had large surface area. This was consistent with SEM results. The large surface area was conducive to the dispersion and adsorption of the active metal as well as improving the catalytic performance of catalysts.

FTIR analysis

FTIR spectra of different samples are shown in Fig. 3.

In the FTIR spectrum of CS, the characteristic broad peak at 3374 cm^{-1} was considered as the stretching vibrations of O–H and N–H in CS.[17–19] The peak observed at 2876 cm^{-1} was ascribed to C–H stretching vibration.[19–21] The weak peak appeared at 1656 cm^{-1} was assigned to the amide C=O stretching.[18,22,23] The weak peak appeared at 1598 cm^{-1} was assigned to the bending band of N–H.[18,23] As shown in the FTIR spectrum of CS, the absorption peak near 1381 cm^{-1} was assigned to deformational vibrations of the –OH group.[19,20] The CS

characteristic band at 1078 cm^{-1} was ascribed to asymmetric stretching vibration of –C–O.[18,23]

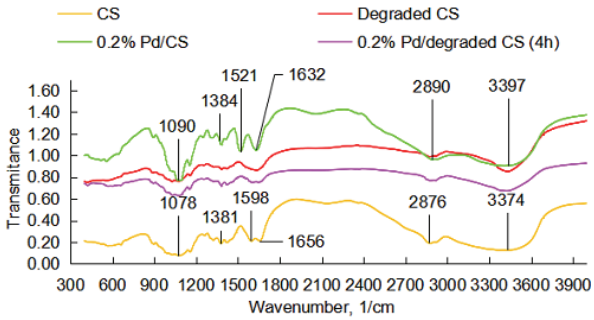

Fig. 3. FTIR spectra of CS, degraded CS (4 h), 0.2 % Pd/CS and 0.2 % Pd/degraded CS (4 h).

Compared with the CS, degraded CS just had some changes in the FTIR spectra, that is, the absorption of O – H and N–H shifted to 3435 cm^{-1} and the absorption of C=O slightly shifted to 1634 cm^{-1}. The absorption peaks at 2876, 1381, 1078 cm^{-1} were almost unchanged. The absorption of of N–H at 1598 cm^{-1} disappeared. These observations proved CS molecule was degraded. The breakage of the CS molecular chains resulted in its structural change. These results indicate that some CS molecular chains were broken from C–NH and C–OH.

Comparison of CS FTIR spectrum with 0.2 % Pd/CS shows that introduction of Pd caused significant changes. The characteristic bands at 3374, 2876 and 1381 cm^{-1} from CS spectrum were also present after Pd loading, but increased slightly in intensity and shifted to 3397, 2890 and 1384 cm^{-1}. Simultaneously, the characteristic bands at 1656, 1598 and 1078 cm^{-1} from CS spectrum were also present after Pd species loading, but varied obviously in intensity and shifted to 1632, 1521 and 1090 cm^{-1}. Coordination of CS with Pd species results in substantial changes of the vibration frequencies.

However, the presence of Pd in degraded CS causes slightly changes in the shape of the FTIR spectra of degraded CS and 0.2 % Pd/degraded CS (4 h). In the FTIR spectrum of degraded CS, the absorb bands at 3435, 2874, 1635, 1387 and 1076 cm^{-1} were shifted to 3425, 2880, 1653, 1385 and 1079 cm^{-1}, respectively. These changes indicate that coordination of the degraded CS with Pd species occurred.

XPS analysis

As listed in Table III, the atomic concentrations of C_{1s}, N_{1s} and O_{1s} of CS are close to that of Pd/CS. However, the contents of C_{1s}, N_{1s} and O_{1s} of CS are different from that of Pd/degraded CS (4 h). The atomic concentration of C_{1s} increased from 65.57 to 79.38 %, while the atomic concentrations of N_{1s} and O_{1s}

decreased from 5.93 and 28.50 % to 1.18 and 19.42 %, respectively. This indicates that part of the CS molecular chains were broken from –OH and –NH during degradation, thus increasing the surface C atom content.

TABLE III. XPS data for Pd/CS, Pd/degraded CS (4 h)

Element	C_{1s}	N_{1s}	O_{1s}	Pd_{3d5}
Compound		CS		
Binding energy[a], eV	285.26	399.04	532.21	–
Atomic concentration, %	65.57	5.93	28.50	–
Compound		Pd/CS		
Binding energy, eV	284.80	399.57	532.87	337.19
Atomic concentration, %	65.11	6.18	28.66	0.05
Chemical state	C–C/C–H	C–N(H)	C–O(H)	Pd–O
Compound		Pd/degraded CS (4 h)		
Binding energy, eV	284.80	399.33	533.29	337.88
Atomic concentration, %	79.38	1.18	19.42	0.02
Chemical state	C–C/C–H	C–N(H)	C–O(H)	PdO*x*

[a]The binding energies were referenced to C_{1s} (284.8eV)

Comparing the XPS data of CS with Pd/CS and Pd/degraded CS (4 h), the binding energy of N_{1s} increased from 399.04 to 399.57 and 399.33 eV, respectively, which indicates that the coordination bonds have formed between Pd and amino group of CS. While the binding energy of O_{1s} rose from 532.21 to 532.87 and 533.29 eV, respectively, indicating that Pd was also coordinated to hydroxyl group of CS. These results were in good agreement with the FTIR results.

As displayed in Table III, the chemical states of Pd in Pd/CS and Pd/degraded CS were PdO and PdO*x*, respectively.

Catalyst performance test

Effect of the Pd load. Taking the degraded CS (6 h) as an example, the effect of Pd load on catalyst performance was studied. The conversion and the selectivity data over Pd/degraded CS (6 h) are shown in Fig. 4.

From Fig. 4a, the conversion enhanced as the temperature increased. The conversion of 0.3 and 0.2 % Pd can achieve 100 % at 150 and 170 °C, respectively. For 0.1 % Pd, acetylene was still not fully converted at 190 °C and the conversion was only 87 %.

In Fig. 4b, the selectivity of 0.1 and 0.2 % Pd varied little with the temperature. However, the selectivity of 0.3 % Pd decreased rapidly with the temperature.

In Fig. 4c, although the selectivity of 0.1 and 0.2 % Pd are as high as 100 % when conversion is less than 22 %, there is no practical significance since the low conversion. When conversion is more than 80 %, the selectivity of 0.3 % Pd

decreases faster. Therefore, the catalyst with 0.2 % Pd has the best compositive property.

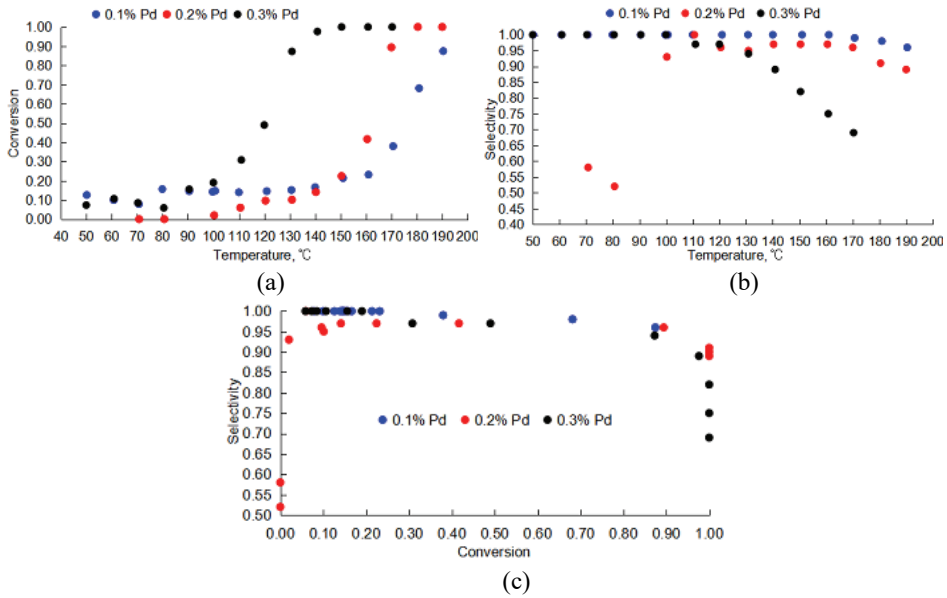

Fig. 4. Effect of the Pd load on catalyst performance: a) the relationship between conversion and temperature; b) the relationship between selectivity and temperature; c) the relationship between selectivity and conversion.

Effect of degradation time. Fig. 5 shows the effect of degradation time on the catalytic performance at 0.2% Pd load.

Fig. 5a shows the change of the conversion with temperature at different degradation times. From Fig. 5a, degradation time had little effect on the conversion below 110 ℃. Above 120 ℃, the conversion of the Pd/degraded CS (4 h) catalyst was significantly higher than that of other catalysts. When the reaction temperature reached 160 ℃, acetylene was completely converted, that is, the conversion of the Pd/degraded CS (4 h) catalyst was 100 %. For the Pd/degraded CS (2 h and 6 h) catalysts, acetylene was completely converted at 190 and 170 ℃, respectively. For the other Pd/degraded CS (0 h, 0.5 h and 1 h) catalysts, the conversions were still below 100 % at 190 °C.

From Fig. 5b, except the selectivity of Pd/degraded CS (0 h, 2 h and 6 h) catalysts was low, there were little differences in the selectivity of the other Pd/degraded CS catalysts. Fig. 5c shows the similar results.

Combining with Fig. 5a and b, it can be concluded that the Pd/degraded CS (4 h) catalyst has the best catalytic effect.

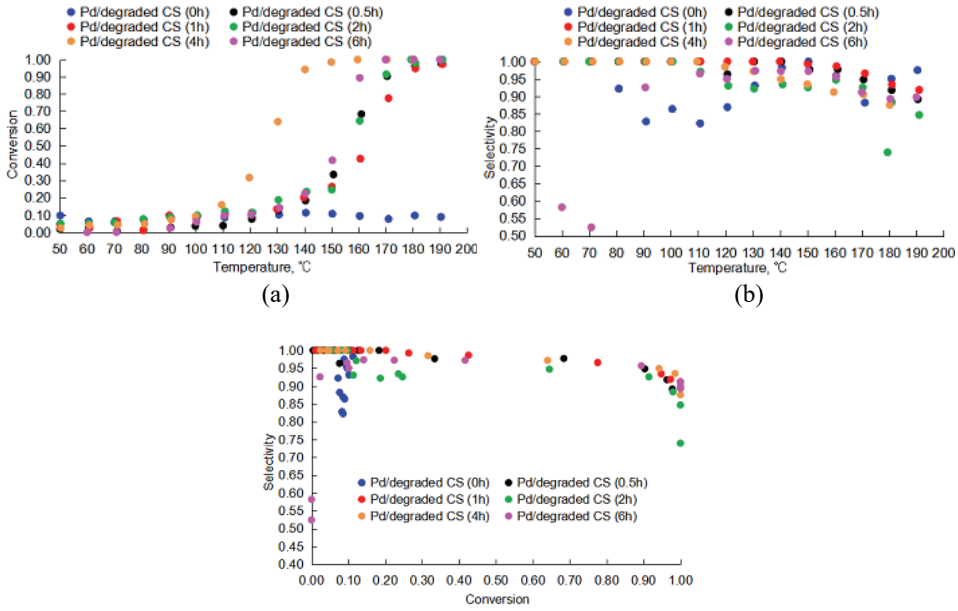

Fig. 5. Effect of degradation time on catalyst performance: a) the relationship between conversion and temperature; b) the relationship between selectivity and temperature; c) the relationship between selectivity and conversion.

Effect of support. Fig. 6 shows the effect of support on the catalytic performance of Pd/CS and Pd/degraded CS (4 h) at 0.2 % Pd load.

As can be seen from Fig. 6a, the conversion of Pd/CS catalyst was lower, the highest conversion was only 11 % in the experimental temperature range. The conversion of Pd/degraded CS (4 h) catalyst was higher than that of Pd/CS. The conversion had reached 94 % at 140 °C and was as high as 100 % at 160 °C.

From Fig. 6b, the selectivity of Pd/CS catalyst was unstable. However, the selectivity of Pd/degraded CS (4 h) showed a regular trend, varying between 100 and 88 %.

From Fig. 6c, the conversion of Pd/CS catalyst was only about 10 %. Such poor conversion has no practical significance.

Therefore, degraded CS (4 h) is more suitable for using as the support of Pd than CS.

Stability of Pd/degraded CS (4 h) catalyst

The stability of a catalyst is very important for industrial application. Hence, the stability of the Pd/degraded CS (4 h) catalyst was tested under the conditions of T = 120 °C, 0.2 % Pd load. Fig. 7 shows the stability results.

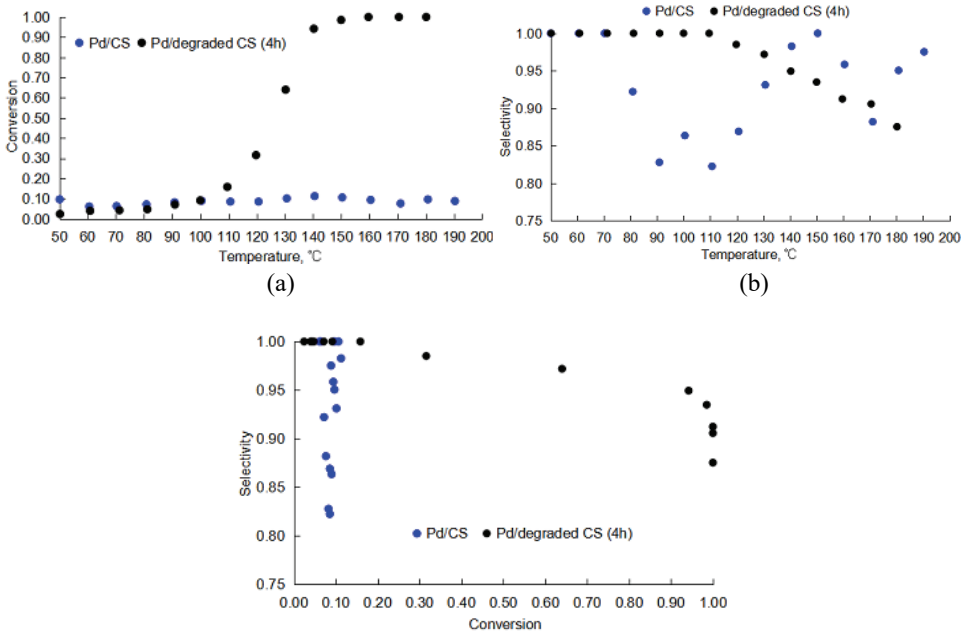

Fig. 6. Effect of support on catalyst performance: a) the relationship between conversion and temperature; b) the relationship between selectivity and temperature; c) the relationship between selectivity and conversion.

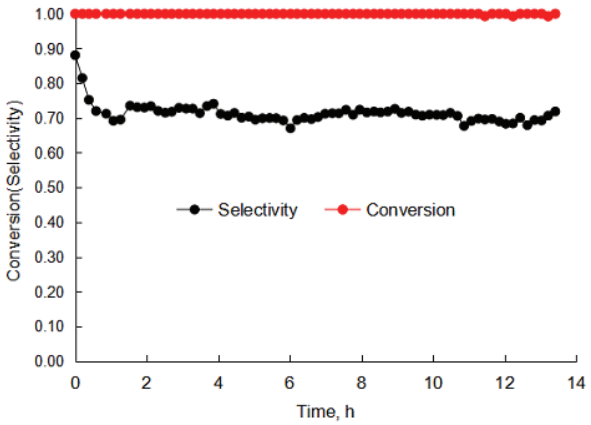

Fig. 7. Acetylene conversion and ethylene selectivity versus time over Pd/degraded CS (4 h) catalyst (T = 120 ℃, 0.2 % Pd load).

As shown in Fig. 7, it is worthy to note that the acetylene conversion over Pd/degraded CS (4 h) remained almost as high as 100 % after 13.5 h. The ethylene selectivity over Pd/degraded CS (4 h) was basically stable at 71 % after 2 h.

During 13.5 h, the ethylene selectivity decreased slightly from 88 to 71 %. These indicate that Pd/degraded CS (4 h) catalyst exhibited good catalytic performance and stability.

CONCLUSIONS

1) CS was successfully degraded in H_2O_2 solution. Degradation of CS made the molecular chain of CS break into small segments. The particle size of degraded CS was much smaller. Pd/degraded CS (4 h) prepared with degraded CS had a larger surface area than Pd/CS prepared with raw CS. Large surface area was more propitious to the dispersion and adsorption of the active metal as well as improving catalytic performance.

2) The results of XRD, FTIR and XPS showed that Pd was successfully coordinated with CS. The chemical states of Pd in Pd/CS and Pd/degraded CS were PdO and PdO*x*, respectively.

3) Among 0.1, 0.2 and 0.3 % Pd load, the Pd/degraded CS (4 h) catalyst with 0.2 % Pd had the best catalytic performance. The conversion and selectivity of Pd/degraded CS (4 h) catalyst could achieve 100 and 91 % at 160 °C, respectively. The low selectivity of conventional Pd-based catalysts was significantly improved.

4) The Pd/degraded CS (4 h) catalyst showed good stability. At lower 120 °C, the acetylene conversion over Pd/degraded CS (4 h) remained almost as high as 100 % and the ethylene selectivity decreased slightly from 88 to 71 % after 13.5 h.

Acknowledgment. This work was supported by National Natural Science Foundation of China (grant number 21476102).

И З В О Д

КАТАЛИТИЧКЕ ПЕРФОРМАНСЕ ПАЛАДИЈУМА/ДЕГРАДИРАНОГ ХИТОЗАНА ЗА СЕЛЕКТИВНУ ХИДРОГЕНАЦИЈУ АЦЕТИЛЕНА

SI-YE TANG[1], XIN-XIANG CAO[1], TONG-TONG DI[2] и XIN-YU LI[3]

[1]College of Chemistry and Chemical Engineering, Luoyang Normal University, Luoyang 471934, China, [2]School of Chemical Engineering, Northwest University, Xian 710069, China и [3]School of Chemical Engineering, Zhengzhou University, Zhengzhou 450001, China

У овом раду испитиване су каталитичке особине катализатора добијених наношењем паладијума на хитозан. Упоређиван је ефекат хитозана и деградираног хитозана на каталитичке перформансе. Структура, морфологија, садржај метала и особине катализатора су испитиване инфрацрвеном спектроскопијом са Фуријеовом трансформацијом, индуктивно спрегнутом плазмом, дифракцијом X-зрачења, нискотемпературском адсорпцијом–десорпцијом N_2 и фотоелектронском спектроскопијом. Резултати су показали да су каталитичке перформансе Pd/деградирани хитозан катализатора боље од Pd/хитозана при одређеним концентрацијама Pd. Катализатор Pd/деградирани хитозан (деградација 4 h) показује одличне каталитичке перформансе и стабилност. Конверзија ацетилена и селективност етилена је достигла 100 и 91 %, редом. У току 13,5 h, конверзија ацетилена је остала 100 %, а селективност етилена је мало опала од 88 до 71 %.

Показано је да је Pd успешно координиран хитозаном; након деградације, честице хитозана постају мање и имају већу специфичну површину; управо су ове честице допринеле побољшању каталитичких перформанси Pd/деградирани хитозан катализатора. Такође, катализатор Pd/деградирани хитозан има високу селективност при високој конверзији, значајно унапређујући карактеристику ниске селективности при високим конверзијама традиционалних катализатора заснованих на Pd.

(Примљено 19. децембра 2024, ревидирано 31. јануара, прихваћено 27. априла 2025)

REFERENCES

1. S. Y. Tang, L. Y. Li, X. X. Cao, Q. Q. Yang, *Heliyon* **9** (2023) e13523 (https://doi.org/10.1016/j.heliyon.2023.e13523)
2. H. Liu, M. Q. Chai, G. X. Pei, X.Y. Liu, L. Li, L. L. Kang, A. Q. Wang, T. Zhang, *Chin. J. Catal.* **41** (2020) 1099 (https://doi.org/10.1016/S1872-2067(20)63568-9)
3. H. Y. Ma, G. C. Wang, *ACS Catal*. **10** (2020) 4922 (https://doi.org/10.1021/acscatal.0c00190)
4. D. Makhmutov, E. Fedorova, A. Zanina, C. Kubis, D. Zhao, D. Doronkin, N. Rockstroh, S. Bartling, U. Armbruster, S. Wohlrab, E. V. Kondratenko, *ACS Catal.* **15** (2025) 2328 (https://doi.org/10.1021/acscatal.4c07462)
5. N. Terzić-Jovanović, V. Ajdačić, *J. Serb. Chem. Soc.* **87** (2022) 669 (https://doi.org/10.2298/JSC220128024T)
6. T. X. Yang, M. Zhao, X. Wang, R. Ma, Y. N. Liu, Y. F. He, D. Q. Li, *Catal. Lett.* **152** (2022) 227 (https://doi.org/10.1007/s10562-021-03620-w)
7. Z. Yang, Y. Li, Y. Cao, X. Zhao, W. Chen, J. Zhang, G. Qian, C. Peng, X. Gong, X. Duan, *Chem. Eng. J.* **445** (2022) 136681 (https://doi.org/10.1016/j.cej.2022.136681)
8. H. Xu, Y. Q. Xu, Y. S. Jiang, Q. F. Zhang, X. N. Li, *Chem. Ind. Eng. Prog*. **38** (2019) 1353 (https://doi.org/10.16085/j.issn.1000-6613.2018-0428) (Chinese)
9. X. Luo, S. B. Guo, D. D. Yu, M. X. Song, F. Zhang, W. P. Fang, W. J. Song, P. F. Ma, W. K. Lai, *Ind. Eng. Chem. Res.* **64** (2025) 2665 (https://doi.org/10.1021/acs.iecr.4c04156)
10. M. Nasrollahzadeh, N. Shafiei, Z. Nezafat, N. S. S. Bidgoli, F. Soleimani, *Carbohydr. Polym.* **241** (2020) 116353 (https://doi.org/10.1016/j.carbpol.2020.116353)
11. H. Y. Luo, D. Y. Liang, Q. Liu, L. Niu, K. Temirlan, W. H. Li, *Carbohydr. Polym.* **354** (2025) 123308 (https://doi.org/10.1016/j.carbpol.2025.123308)
12. E. Guibal, *Prog. Polym. Sci.* **30** (2005) 71 (https://doi.org/10.1016/j.progpolymsci.2004.12.001)
13. S. Zhong, *Kin. Catal.* **61** (2020) 480 (https://doi.org/10.1134/S0023158420030210)
14. K. X. Li, X. F. Song, D. Zhang, *J. Appl. Polym. Sci.* **109** (2008) 1294 (https://doi.org/10.1002/app.28186)
15. X. X. Cao, T. T. Lu, W. T. Xie, M. Arash, B. Adelaide, H. Ricky, W. L. J. Ben, K. K. Jong, M. Karren, C. J. Liu, X. L. Yan, *Front. Chem. Sci. Eng.* **14** (2020) 522 (https://doi.org/10.1007/s11705-019-1822-3)
16. S. Shawe, F. Buchanan, E. Harkin-Jones, D. Farrar, *J. Mater. Sci.* **41** (2006) 4832 (https://doi.org/10.1007/s10853-006-0064-1)
17. J. Li, C. P. Wei, F. M. Wang, L. D. Dong, S. Sun, Q. Y. Liu, *Mater. Sci. Forum* **852** (2016) 1319 (https://doi.org/10.4028/www.scientific.net/MSF.852.1319)
18. T. Baran, A. Menteş, H. Arslan, *Int. J. Biol. Macromol.* **72** (2015) 94 (https://doi.org/10.1016/j.ijbiomac.2014.07.029)

19. N. V. Kramareva, A. E. Koklin, E. D. Finashina, N. S. Telegina, A. Yu. Stakheev, L. M. Kustov, *Kinet. Catal.* **45** (2004) 743 (https://doi.org/10.1023/B:KICA.0000044989.54767.b4)
20. X. Li, K. Cui, Z. Guo, T. Yang, Y. Cao, Y. Xiang, H. Chen, M. Xi, *Chem. Eng. J.* **379** (2020) 122324 (https://doi.org/10.1016/j.cej.2019.122324)
21. N. Anbu, R. Maheswari, V. Elamathi, P. Varalakshmi, A. Dhakshinamoorthy, *Catal. Commun.* **138** (2020) 105954 (https://doi.org/10.1016/j.catcom.2020.105954)
22. I. M. El-Sherbiny, *Eur. Polym. J.* **45** (2009) 199 (https://doi.org/10.1016/j.eurpolymj.2008.10.042)
23. T. Baran, A. *Mentes¸*, *Int. J. Biol. Macromol.* **79** (2015) 542 (http://dx.doi.org/10.1016/j.ijbiomac.2015.05.021).